

INELASTIC FINAL STATE INTERACTIONS IN B DECAYS TO TWO PSEUDOSCALAR MESONS*

P. ŻENCZYKOWSKI

Dept. of Theoretical Physics, H. Niewodniczański Institute of Nuclear Physics
Radzikowskiego 152, 31-342 Kraków, Poland
e-mail: zenczyko@iblis.ifj.edu.pl

(Received September 15, 2003)

We present first results of an approach in which all contributions from Zweig-rule-satisfying $SU(3)$ -breaking final-state interactions (FSIs) in $B \rightarrow PP$ decays are taken into account. We include the effects due to Pomeron exchange between the two outgoing pseudoscalar mesons, neglect charmed intermediate states, and express all of the other rescattering effects in terms of only three effective complex parameters. It is pointed out that the experimental bound on the $B \rightarrow K^+K^-$ branching ratio limits the value of only one of these parameters, thus permitting sizable FSI effects in other B decays. From the fits to the experimental $B \rightarrow PP$ branching ratios we determine the values of the FSI parameters and the weak angle γ . A broad range of around 60° – 100° is admitted for the latter, which includes the region expected in the Standard Model.

PACS numbers: 13.25.Hw, 11.30.Hv, 12.15.Hh, 11.80.Gw

1. Introduction

Most analyses of CP-violating effects in B decays are based on short-distance (SD) amplitudes only. In other words, any possible final-state interactions (FSIs) are usually completely neglected. While it is very difficult to assess if this neglect is justified or not, various authors have argued that FSIs should be important and, consequently, that reliable analyses of B decays must take these interactions (and the inelastic ones in particular) into account [1–5].

Since a direct calculation of the effects of all inelastic FSIs is beyond our means, an $SU(3)$ -symmetric approach was developed [6,7], in which the sum

* Presented at the XLIII Cracow School of Theoretical Physics, Zakopane, Poland, May 31–June 9, 2003.

of *all* such effects is expressed in terms of only three *effective* complex parameters. The approach has been recently extended to include SU(3)-symmetry-breaking effects [8]. Below we shall briefly review the whole scheme, along with its most important results.

In the following section we specify the SD input used. In Section 3 we give a brief description of our treatment of all FSIs. Section 4 is devoted to the presentation of the fits performed within our approach and a short discussion of our results. Our main conclusions are reiterated in Section 5.

2. Short-distance parameters

SD amplitudes for B decays are customarily expressed in terms of SD quark-diagram amplitudes of different topologies: T (tree), P (penguin), C (color-suppressed), S (singlet penguin), *etc.* The relevant amplitudes may be strangeness-conserving (for $b \rightarrow d u \bar{u}$ decays), and strangeness-violating (for $b \rightarrow s u \bar{u}$ decays). As usual, we distinguish the strangeness-violating quark-diagram amplitudes by a prime. The dominant SD amplitudes are then, in order of their importance: $T \gg P \approx C$ ($P' > S' \gg T' > C'$) in strangeness-conserving (strangeness-violating) sections.

For our study of the effect of FSIs to be feasible, we must bring down the number of SD and FSI parameters as much as possible. Therefore, we assume first that the strong SD phases are negligible. (In Ref. [9] these phases were of the order of 10° , while in Ref. [10] it is argued that the FSI-uncorrected amplitudes do not contain any strong phases).

Further reduction of the number of SD parameters follows from the assumption of the following (SU(3)-breaking) relations between the SD quark-diagram amplitudes:

1. for tree amplitudes

$$T' = |T'|e^{i\gamma} = \frac{V_{us} f_K}{V_{ud} f_\pi} T \approx 0.276 T, \quad (1)$$

2. for penguin amplitudes (dominated by the t quark, hence the weak phase factor being $e^{-i\beta}$ for P , and ± 1 for P' , *i.e.* $P' = \pm|P'|$)

$$P = -e^{-i\beta} \left| \frac{V_{td}}{V_{ts}} \right| P' \approx -0.176 e^{-i\beta} P', \quad (2)$$

3. for color-suppressed amplitudes

$$C = \xi T \quad (3)$$

and

$$C' = T'(\xi - (1 + \xi)\delta_{\text{EWE}}^{-i\gamma}), \quad (4)$$

where we take $\xi = \frac{C_1 + \zeta C_2}{C_2 + \zeta C_1} \approx 0.17$ (see [8]), and include the contribution from the electroweak penguin P'_{EW} (described by $\delta_{EW} \approx +0.65$ [11]), with all other electroweak penguins neglected,

4. singlet penguin amplitude (with weak phase equal 0, as for P') is independent of other SD amplitudes (the data require that this amplitude be sizable [12, 13]),
5. other quark-diagram amplitudes are assumed negligible.

In the fits described in Section 4 we accept $\beta = 24^\circ$, which is in agreement with the world average [14] $\sin 2\beta = 0.734 \pm 0.054$. Consequently, SD amplitudes are parametrized by four parameters: $|T|$, P' , S' , and the weak phase γ .

3. Simplified description of FSI

Under the assumption that FSIs are independent of the original SD decay mechanism, the set of all FSI-corrected weak decay amplitudes $\mathbf{W} \equiv \{W_k\}$ may be expressed as:

$$\mathbf{W} = \mathbf{S}^{1/2} \mathbf{w} \equiv \mathbf{w} - \mathbf{a}\mathbf{w} + i\Delta\mathbf{W}_{\text{inel}}, \tag{5}$$

where \mathbf{w} represents the set of all SD decay amplitudes $\{w_k\}$, \mathbf{S} is the strong interaction S-matrix; the terms $-\mathbf{a}\mathbf{w}$ (with $(\mathbf{a}\mathbf{w})_k \equiv a_k w_k$) and $i\Delta\mathbf{W}_{\text{inel}}$ represent the Pomeron-exchange-induced corrections, and the “inelastic” FSI corrections (including the $P_1 P_2 \rightarrow P_1 P_2$ elastic transitions not mediated by Pomeron) respectively. The Pomeron-mediated FSIs involve no parameters and are directly calculable. For exact SU(3), the exchange of Pomeron leads to overall renormalization of the SD amplitudes only. Thus, only the SU(3)-breaking part of Pomeron-mediated interactions may modify the pattern of SD amplitudes.

The main problem is the treatment of inelastic FSIs. Consequently, several simplifications have to be introduced (for more details see [6, 7, 15]). These are:

1. All intermediate inelastic states are represented by quasi-two-body states $M_1 M_2$, as the SD decay process always produces two quark-antiquark pairs at the most (see [7]).
2. SD amplitudes $w_X(B \rightarrow M_1 M_2)$, corresponding to a given quark diagram X ($X \rightarrow P, T, \text{etc.}$) and a given final state $M_1 M_2$, are assumed to be proportional to the SD $w_X(B \rightarrow PP)$ amplitudes for a diagram of the same topology and with a similar flavor composition of the

PP state, with the (unknown) proportionality coefficients $\eta(M_1M_2)$ depending only on the M_1M_2 state produced:

$$w_X(B \rightarrow M_1M_2) = \eta(M_1M_2)w_X(B \rightarrow PP). \tag{6}$$

Complete SD amplitudes are given as sums over their contributing diagrams. With the above assumptions, the FSI-corrected amplitudes \mathbf{W} are given in terms of quark-diagram SD amplitudes $P, T, \text{etc.}$, and various FSI parameters. Even for exactly $SU(3)$ -symmetric FSIs, the number of independent and — in principle — measurable data in all $B \rightarrow PP$ decays turns out to be too small to determine all of these parameters [6, 7].

3. In order to limit the number of rescattering parameters, the Zweig rule and nonet $SU(3)$ symmetry for intermediate states are additionally assumed [7]. Let us consider the $SU(3)$ -symmetric FSIs first. Then, there are just two possible topologies of quark-line diagrams (Fig. 1), to which only three possible $SU(3)$ structures (hence three complex pa-

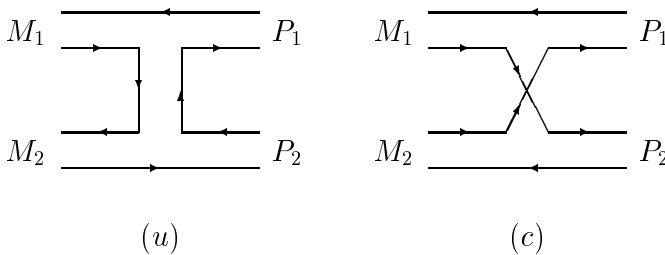


Fig. 1. Types of rescattering diagrams: (u) uncrossed, (c) crossed.

rameters) may be assigned. The uncrossed FSI diagrams of Fig. 1(u) are parametrized with the help of parameters u_+ and u_- , corresponding to the $SU(3)$ -invariant forms:

$$\begin{aligned} & \text{Tr}(\{M_1^\dagger, M_2^\dagger\}\{P_1, P_2\}) u_+, \\ & \text{Tr}([M_1^\dagger, M_2^\dagger]\{P_1, P_2\}) u_-. \end{aligned} \tag{7}$$

The first (second) structure describes transitions in which the product of charge conjugation parities of mesons M_1 and M_2 is positive (negative), *i.e.* $C_{M_1} \cdot C_{M_2} = +1(-1)$, respectively. For the crossed diagrams of Fig. 1(c), only one $SU(3)$ structure is possible:

$$\text{Tr}(M_1^\dagger P_1 M_2^\dagger P_2 + M_1^\dagger P_2 M_2^\dagger P_1) c. \tag{8}$$

The other structure, with a “−” sign in between the two terms above, is inconsistent with the requirements of Bose symmetry for the final PP state.

The FSI-corrected amplitudes \mathbf{W} may be expressed in terms of FSI-corrected quark-diagram amplitudes, denoted here as \tilde{T} , \tilde{C} , \tilde{P} , \tilde{S} , \tilde{A} (annihilation), \tilde{E} (exchange), and $\tilde{P}A$ (penguin annihilation). In the case of SU(3)-symmetric FSIs, their relation to the input SD amplitudes T , C , P , and S is [7]:

$$\begin{aligned} \tilde{T} &= T + C \cdot 2c, \\ \tilde{C} &= C + T \cdot 2c, \\ \tilde{P} &= P + S \cdot (2c + 2u) + (T + 3P + S) \cdot d, \\ \tilde{S} &= S + P \cdot 2c, \\ \tilde{A} &= C \cdot 2u, \\ \tilde{E} &= T \cdot 2u, \\ \tilde{P}A &= 2P \cdot 2u, \end{aligned} \tag{9}$$

where

$$u = \frac{u_+ + u_-}{2}, \tag{10}$$

$$d = u_+ - u_-. \tag{11}$$

From Eq. (9) we see that the size of long-distance penguins generated by the FSIs from the tree diagrams is controlled by the d parameter.

4. Theory and experiments suggest that SU(3) is broken via a suppression of those amplitudes in which a strange quark is exchanged between the M_1 and M_2 mesons of the original pair. The above SU(3)-invariant forms (Eqs. (7), (8)) may be modified appropriately to take this suppression into account [8]. This requires the introduction of additional parameter(s). The dependence between the input SD quark-diagram amplitudes and the FSI-corrected amplitudes cannot then be reduced to a simple form similar to that given in Eq. (9). The relevant formulas are given in Ref. [8]. The studies performed in [8] show that the best fits to the $B \rightarrow PP$ branching ratios are obtained when SU(3) in these FSIs is strongly broken. Consequently, in Section 4 below we present only those results of [8] which are obtained when the limit of maximally broken SU(3) is taken. For the case of maximally broken SU(3), some of the most interesting FSI corrections are gathered in Table I. In order to hide the SU(3)-symmetric part of Pomeron-mediated FSI into our parameters, we introduced there:

$$\bar{u} = \frac{u}{1 - a(\pi\pi)}, \tag{12}$$

$$\bar{d} = \frac{d}{1 - a(\pi\pi)}, \tag{13}$$

$$\bar{T} = T(1 - a(\pi\pi)), \tag{14}$$

$$\bar{P} = P(1 - a(\pi\pi)), \tag{15}$$

$$\dots, \tag{16}$$

where $a(\pi\pi)$ (directly calculable to be 0.16) describes Pomeron-mediated FSIs in the $\pi\pi$ channel. Furthermore,

$$\begin{aligned} \Delta &= (2\bar{P} + \bar{T}) \bar{d}, \\ \Delta' &= (2\bar{P}' + \bar{T}') \bar{d}. \end{aligned} \tag{17}$$

TABLE I

Selected rescattering contributions to $B^+, B_d^0 \rightarrow PP$ decays for inelastic FSI with maximally broken SU(3): $\Delta \equiv (2\bar{P} + \bar{T}) \bar{d}$; $\Delta' \equiv (2\bar{P}' + \bar{T}') \bar{d}$.

Decay	uncrossed FSI diagrams	crossed FSI diagrams
$B^+ \rightarrow \pi^+ \pi^0$	0	$-\frac{1}{\sqrt{2}} 2\bar{c}(\bar{T} + \bar{C})$
$K^+ \bar{K}^0$	0	0
$B_d^0 \rightarrow \pi^+ \pi^-$	$-(\Delta + 2\bar{u}(\bar{T} + 2\bar{P}))$	$-2\bar{c}\bar{C}$
$\pi^0 \pi^0$	$\frac{1}{\sqrt{2}}(\Delta + 2\bar{u}(\bar{T} + 2\bar{P}))$	$-\frac{1}{\sqrt{2}} 2\bar{c}\bar{T}$
$K^+ K^-$	$2\bar{u}\bar{P}$	0
$K^0 \bar{K}^0$	$-2\bar{u}\bar{P}$	0
$B^+ \rightarrow \pi^+ K^0$	$-\Delta' - 2\bar{u}(\bar{C}' + \bar{S}')$	$-\bar{c}\bar{S}'$
$\pi^0 K^+$	$\frac{1}{\sqrt{2}}(\Delta' + 2\bar{u}(\bar{C}' + \bar{S}'))$	$\frac{1}{\sqrt{2}}\bar{c}(\bar{T}' + \bar{C}' + \bar{S}')$
$B_d^0 \rightarrow \pi^- K^+$	$\Delta' + 2\bar{u}\bar{S}'$	$\bar{c}(\bar{C}' + \bar{S}')$
$\pi^0 K^0$	$-\frac{1}{\sqrt{2}}(\Delta' + 2\bar{u}\bar{S}')$	$\frac{1}{\sqrt{2}}\bar{c}(\bar{T}' - \bar{S}')$

4. Fits and their results

We performed fits to the available branching ratios of B decays, comparing the situation with no FSI (*i.e.* for $\mathbf{W} = \mathbf{w}$ only) to the following two cases:

- (a) SU(3)-breaking Pomeron-exchange-induced FSIs only (*i.e.* with $\mathbf{W} = \mathbf{w} - \mathbf{aw}$ and SU(3)-breaking \mathbf{a});
- (b) both Pomeron-exchange-induced and non-Pomeron inelastic SU(3)-breaking FSIs (*i.e.*, with full \mathbf{W} of Eq. (5)).

As an input for the fits only the branching ratios of the $B \rightarrow PP$ decays were taken into account. The fit procedure consisted in minimizing the sum over 16 decay channels i of the deviations between the experimental and theoretical branching ratios \mathbf{B}_i normalized to their experimental errors (see *e.g.* [9, 16]):

$$f(\text{SD ampl; FSI param.}) = \sum_i \frac{(\mathbf{B}_i(\text{theor}) - \mathbf{B}_i(\text{exp}))^2}{(\Delta \mathbf{B}_i(\text{exp}))^2}. \quad (18)$$

For details of the fit procedures and their results, see [8]. In the fits we used not only the $B \rightarrow \pi\pi$ and $B \rightarrow \pi K$ branching ratios (as in [9, 16]), but also those of $B \rightarrow K\eta, K\eta'$ *etc.*, not considered elsewhere. Inclusion of the latter (mandatory for a complete description of FSI) was possible thanks to the introduction of the singlet penguin amplitude S' as an additional parameter.

4.1. Pomeron-exchange-induced FSIs

For the no-FSI case, the fit to all 16 decay channels (which include $\pi\eta(\eta')$ and $K\eta(\eta')$ channels) yields $\gamma = 103^\circ$, in agreement with earlier fits to the $B \rightarrow \pi\pi, \pi K$ branching ratios preferring $\gamma \gtrsim 90^\circ$ [9, 16, 17]. When SU(3)-breaking Pomeron-exchange-induced FSIs are taken into account, the best fit to the data is obtained for $P' < 0$ and $\gamma = 101^\circ$. The dependence of the minimized function f on γ is shown in Fig. 2. Solid lines correspond to no FSIs (or to fully SU(3)-symmetric Pomeron-exchange-induced FSIs); dashed lines correspond to SU(3)-breaking Pomeron-induced FSIs. Clearly, inclusion of SU(3)-breaking in Pomeron-mediated FSI cannot bring the fitted value of γ into agreement with the Standard Model expectations of $\gamma_{\text{SM}} \approx 64.5^\circ \pm 7^\circ$ [17].

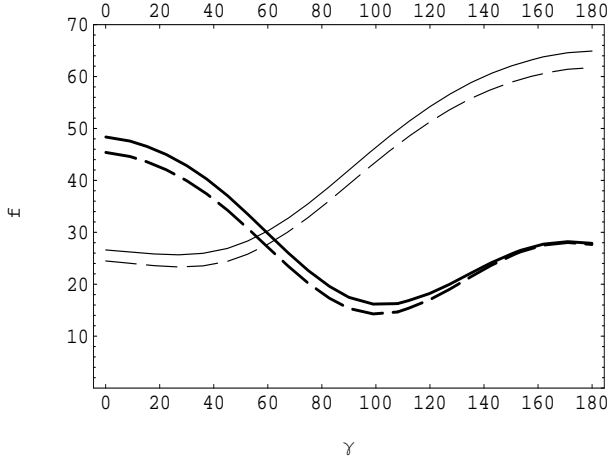


Fig. 2. Dependence of minimized function f (Eq. (18)) on γ : thin lines — $P' > 0$, thick lines — $P' < 0$; solid lines — no FSIs / SU(3) symmetric Pomeron-induced FSIs, dashed lines — SU(3)-breaking Pomeron-induced FSIs.

4.2. Full FSIs

The FSI parameters were further restricted by the following considerations:

1. Since the present upper bound on the value of the $B_d^0 \rightarrow K^+K^-$ branching ratio ($< 0.6 \times 10^{-6}$) limits the size of \bar{u} quite severely (*cf.* Table I), $\bar{u} = 0$ was assumed in the fits.
2. Since for $\bar{u} = 0$, the FSI-induced corrections vanish for all $B^+, B_d^0 \rightarrow K\bar{K}$ decays (Table I), the branching ratios of the $B \rightarrow K\bar{K}$ decays cannot yield any restrictions on the values of \bar{d} and \bar{c} which must be treated as free parameters. However, \bar{c} should be real as the s -channel in Fig. 1(c) is exotic.

Thus, all inelastic FSI effects are ultimately parametrized in terms of only three real parameters ($\text{Re } \bar{d}$, $\text{Im } \bar{d}$, $\text{Re } \bar{c} = \pm|\bar{c}|$).

First we considered the two limiting cases when $|\bar{d}| \ll |\bar{c}|$ and $|\bar{d}| \gg |\bar{c}|$, assuming $\bar{d} = 0$ and $\bar{c} = 0$, respectively. The results of the two fits for the $P' < 0$ case are shown in Fig. 3 as a function of γ (for the $P' > 0$ case, the minimum is much higher). Solid (dashed) lines correspond to $\bar{d} = 0$ ($\bar{c} = 0$), respectively. Since the FSI contributions should constitute only corrections to the SD expressions, the value of \bar{d} was additionally bounded by $|\text{Re } \bar{d}| < 0.25$, $|\text{Im } \bar{d}| < 0.25$. Restricting the size of $|\bar{c}|$ was not necessary. For more details see Ref. [8].

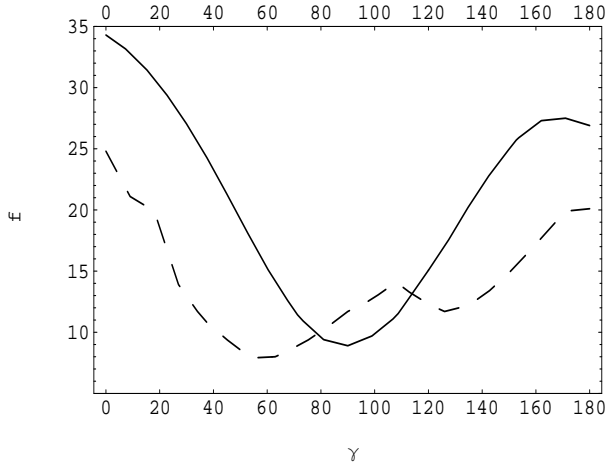


Fig. 3. Dependence of minimized function f (Eq. (18)) on γ for full FSI with $P' < 0$; solid lines — $\bar{d} = 0$, unrestricted $|\bar{c}|$; dashed lines — $\bar{c} = 0$, $|\text{Re } \bar{d}| < 0.25$, $|\text{Im } \bar{d}| < 0.25$.

Comparison with Fig. 2 shows that in both limiting cases the inclusion of inelastic FSI permits a substantial reduction of f when compared to the no-FSI case (from 14.0 down to around 8.0). Furthermore, the fitted value of γ appears now significantly shifted. For $\bar{d} = 0$ the shift is from 102° to around 90° , with $\bar{c}_{\text{fit}} = 0.24$ (Fig. 3, solid line); while for $\bar{c} = 0$ the fit yields $\gamma = 57^\circ$, with $\text{Re } \bar{d}_{\text{fit}} \approx -0.22$ and $\text{Im } \bar{d}_{\text{fit}} \approx +0.21$ (Fig. 3, dashed line). The corresponding fitted values of SD amplitudes were: $\bar{T} = 2.41(2.71)$, $\bar{P}' = -4.24(-6.17)$, $\bar{S}' = -2.09(-1.53)$ for $\bar{d} = 0$ ($\bar{c} = 0$), respectively.

In the most general fit, all three FSI parameters ($\text{Re } \bar{d}$, $\text{Im } \bar{d}$, \bar{c}) were free. It turns out (see [8]) that the overall minimum is then very close to the point $\text{Re } \bar{d} = -0.22$, $\text{Im } \bar{d} = +0.21$, $\bar{c} = 0$ discussed previously. A more detailed study shows [8] that for all values of γ in the region of $80^\circ \pm 20^\circ$ or so, the obtained values of f (with appropriately fitted \bar{d} and \bar{c}) are in the region of 8.5 ± 1 . Taking into account that our approach is of necessity highly simplified, a difference of 1 in f cannot be treated as meaningful. Consequently, all γ from around 60° to 100° are admitted by the fits. To sum up, our results show that the inclusion of inelastic FSI effects significantly diminishes the value of the minimized function f and may help in bringing the extracted value of γ down to the SM range [17].

For negligible strong SD phases, it is the third term in Eq. (5) which allows the existence of direct CP violation effects. This term provides a specific prescription for how strong phases are generated by quark interchanges between outgoing mesons. For $\bar{u} = 0$, the pattern of FSI phases in all $B \rightarrow PP$

decays, and hence the pattern of CP-violating observables is governed by parameters \bar{d} , \bar{c} . For a given value of γ , the values of these parameters are fixed by the fit to the branching ratios, with the subsequent calculation of CP-violating observables being unambiguous and straightforward. The resulting asymmetries depend upon the value of γ in a distinguishable manner. As experimental data on relevant asymmetries are still not precise, it is too early to draw definite conclusions from any (dis)agreement of our approach with the data. However, it should be mentioned that, with the exception of the $B^+ \rightarrow \pi^+\eta$ asymmetry measurement (difficult to accommodate in any approach, see [18]), other CP asymmetries (*i.e.* for $B \rightarrow K\pi$, and $K^+\eta(\eta')$) and the time-dependent rates in $B_d^0(t) \rightarrow \pi^+\pi^-$ weakly hint at the SM value of γ (see [8]).

5. Conclusions

We have presented the first quantitative and complete treatment of all inelastic FSIs in B decays to two light pseudoscalar mesons. The only neglected but potentially important corrections were those due to the intermediate states composed of charmed mesons. Our main conclusions are:

1. Small size of the experimental $B_d^0 \rightarrow K^+K^-$ branching ratio *does not imply* that inelastic rescattering effects in other $B \rightarrow PP$ decays may be neglected, the reason being that the $B_d^0 \rightarrow K^+K^-$ decay amplitude does not depend on parameters describing the long-distance u -loop penguin and the FSI-induced quark rearrangement.
2. Our fits permit the values of γ in the range of 60° – 100° or so, and weakly hint at γ values compatible with SM expectations. Thus, the FSIs may help in bringing the extracted value of γ down to the Standard Model range.

Better data and further analysis of FSI effects (including the role of charming penguins) are needed before one could safely conclude that the overall body of data on $B \rightarrow PP$ decays favors the SM value of γ .

REFERENCES

- [1] L. Wolfenstein, *Phys. Rev.* **D43**, 151 (1991); M. Suzuki, L. Wolfenstein, *Phys. Rev.* **D60**, 074019 (1999).
- [2] J.F. Donoghue, E. Golowich, A.A. Petrov, J.M. Soares, *Phys. Rev. Lett.* **77**, 2178 (1996); P. Żenczykowski, *Acta Phys. Pol. B* **28**, 1605 (1997); M. Neubert, *Phys. Lett.* **B424**, 152 (1998).

- [3] W.S. Hou, K.C. Yang, *Phys. Rev. Lett.* **84**, 4806 (2000).
- [4] P. Żenczykowski, *Phys. Rev.* **D63**, 014016 (2001); *Acta Phys. Pol. B* **32**, 1847 (2001).
- [5] J.-M. Gerard, J. Weyers, *Eur. Phys. J.* **C7**, 1 (1999); D. Atwood, A. Soni, *Phys. Rev.* **D58**, 036005 (1998); A. Falk, A. Kagan, Y. Nir, A. Petrov, *Phys. Rev.* **D57**, 4290 (1998).
- [6] P. Żenczykowski, *Acta Phys. Pol. B* **33**, 1833 (2002).
- [7] P. Łach, P. Żenczykowski, *Phys. Rev.* **D66**, 054011 (2002).
- [8] P. Żenczykowski, P. Łach, [hep-ph/0309198](https://arxiv.org/abs/hep-ph/0309198).
- [9] M. Beneke, G. Buchalla, M. Neubert, C.T. Sachrajda, *Nucl. Phys.* **B606**, 245 (2001)
- [10] J.-M. Gerard, C. Smith, *Eur. Phys. J.* **C30**, 69 (2003).
- [11] M. Neubert, J.L. Rosner, *Phys. Lett.* **B441**, 403 (1998).
- [12] A.S. Dighe, M. Gronau, J.L. Rosner, *Phys. Rev. Lett.* **79**, 4333 (1997).
- [13] C.W. Chiang, J.L. Rosner, *Phys. Rev.* **D65**, 074035 (2002).
- [14] Y. Nir, *Nucl. Phys. Proc. Suppl.* **117**, 111 (2003).
- [15] P. Żenczykowski, *Acta Phys. Pol. B* **34**, 4435 (2003).
- [16] A. Höcker, H. Lacker, S. Laplace, F. Le Diberder, *Eur. Phys. J.* **C21**, 225 (2001).
- [17] M. Battaglia *et al.*, [hep-ph/0304132](https://arxiv.org/abs/hep-ph/0304132).
- [18] C.-W. Chiang, M. Gronau, J.L. Rosner, [hep-ph/0306021](https://arxiv.org/abs/hep-ph/0306021).